GUIDANCE AND CONTROL 1986

Edited by
Robert D. Culp
John C. Durrett

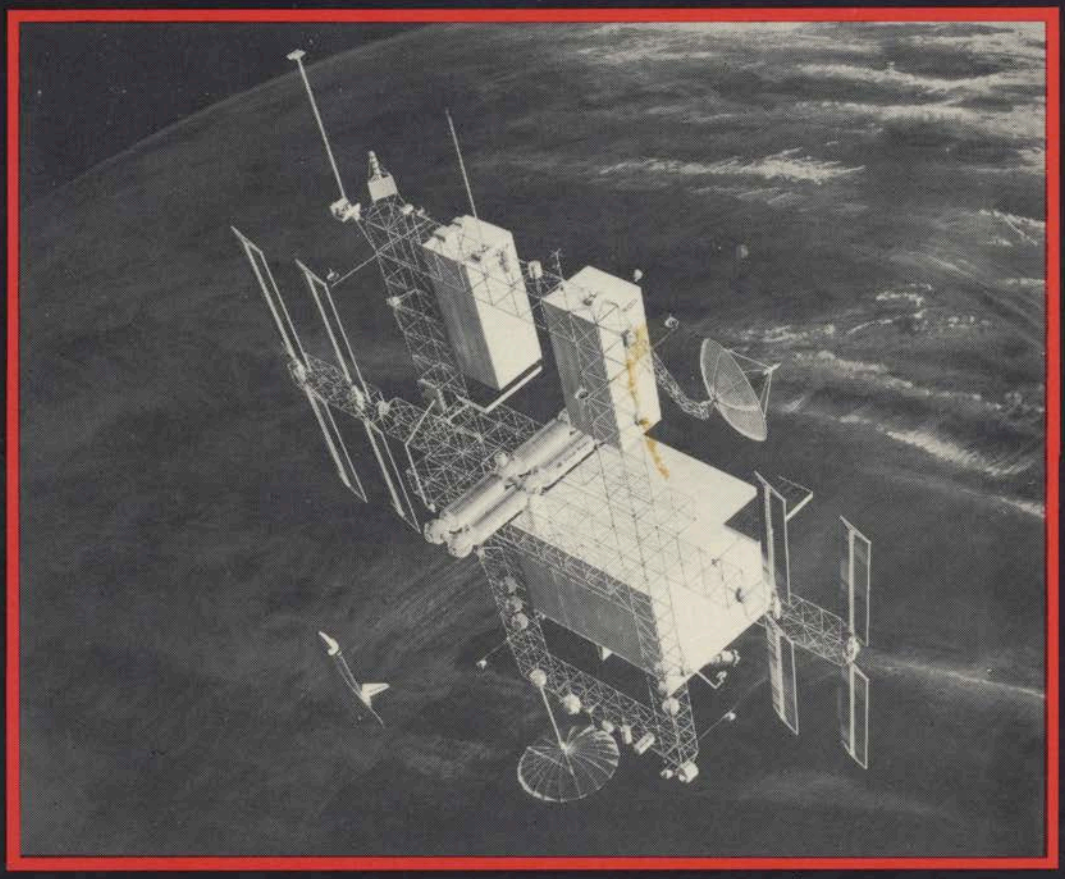

Volume 61
ADVANCES IN THE ASTRONAUTICAL SCIENCES

AN AMERICAN ASTRONAUTICAL SOCIETY PUBLICATION

AAS 86-036

A HIGHLY ADAPTABLE STEERING/SELECTION PROCEDURE FOR COMBINED CMG/RCS SPACECRAFT CONTROL

Joseph A. Paradiso*

Linear Programming techniques have been applied to develop a CMG steering law which exhibits very high adaptability to CMG hardware failures and variations in CMG system definition. The procedure is also capable of performing a fuel-optimal jet selection and establishing control via a hybrid mixture of jets and CMGs. This report presents the structure of the hybrid steering/selection principle and illustrates its performance through a set of simulation examples.

INTRODUCTION

Attitude control and momentum management of the space station will be realized primarily by Control Moment Gyroscopes (CMGs) and Reaction Control System (RCS) jets. The space station environment will be very dynamic; its characteristics will evolve dramatically during buildup, and significant changes in mass properties and actuator response can be expected during routine operations. Control, steering, and actuator selection procedures must be able to provide an adaptive response in order to function effectively under these conditions. Existing CMG steering laws, however, are often subject to restrictions which may be significantly disadvantageous for applications such as space station.

CMG steering laws can frequently become considerably calculation-intensive, and attempts at simplification generally result in tight restrictions being placed upon the CMG system configuration and behavior. This reduces available degrees of freedom and greatly lowers the ability of the system to deal with device failures and changes in the CMG definition.

Present steering laws generally calculate CMG gimbal rates via a pseudo-inverse method, which requires an additional "Null Motion"

* *Technical Staff, Control & Dynamics Division, C.S. Draper Laboratory, 555 Technology Square, Cambridge, Massachusetts 02139.*

procedure to compute gimbal commands that prevent the CMGs from being driven into stable singular states. Pseudo-inverse formulations are not readily conducive to changes in the number of available actuators; when adding or deleting CMGs, the dimension of the pseudo-inverse and related calculations must be correspondingly adjusted.

Peak limits on CMG output torque and stop constraints on gimbal excursion are not considered in most CMG steering procedures and must be enforced after the CMG selection has been performed.

Current spacecraft systems possessing jets and CMGs employ independent jet selection and CMG steering procedures. This strategy generally does not enable operation both sets of actuators in a coordinated fashion. The space station environment, however, encourages a control scheme which addresses the possibility of mixed CMG/RCS response, particularly in the cases of re-boost, desaturation, docking, or other maneuvers in which the CMGs are saturated or do not possess sufficent control authority to satisfy input requests without assistance from other actuators.

The effort summarized in this report has addressed the problems posed above, and has resulted in an efficent and extremely flexible CMG steering algorithm. The actuator selection process is not limited to CMGs; the same procedure is used to perform fuel-optimal jet selections and control spacecraft via a hybrid mixture of jets and CMGs.

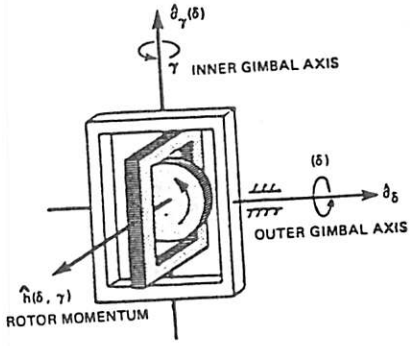

FIGURE 1: DOUBLE-GIMBALLED CMG

LINEAR SELECTION AND STEERING

CMGs are momentum exchange devices which create an output torque by changing the orientation of angular momentum stored in a rotor spinning at constant rate. An Euler-mounted double-gimballed CMG (as assumed in this analysis) is sketched in Fig. 1. Given sufficent gimbal freedom, this device is capable of projecting its angular momentum along any arbitrary axis.

The total angular momentum of a spacecraft and its complement of CMGs is constant in the absence of external torques; any change in the momentum state of the CMG system is transferred to the spacecraft. Quantitatively:

$$\underline{H}_s + \sum_{CMGs} \underline{h}_i = \text{constant} \tag{1}$$

$$\frac{\partial \underline{H}_s}{\partial t} + \underline{\omega}_s \times \underline{H}_s = -\frac{\partial \Sigma \underline{h}_i}{\partial t} = -\underline{\omega}_s \times \sum_{CMGs} \underline{h}_i + \sum_{CMGs} \underline{\tau}_{ctl_i} \tag{2}$$

$\underline{H}_s$ = Angular momentum of spacecraft
$\underline{\omega}_s$ = Spacecraft angular rate
$\underline{h}_i$ = Angular momentum stored in CMG rotor i

Eq. (2) defines the torque applied to the spacecraft by the CMG system. It is derived by taking the time derivative of Eq. (1) with respect to spacecraft-fixed coordinates. The "$\underline{\omega}_s \times \underline{H}_s$" term on the leftmost side of Eq. (2) is due to Euler coupling of spacecraft axes and does not arise from the presence or action of CMGs, thus is ignored in this analysis.

Both terms on the right-hand side of Eq. (2) are caused by changes in the stored CMG momentum. The first term originates from rotation of the CMGs relative to inertial space as they are carried along by the spacecraft angular rate. This term can be directly subtracted from the torque command input to the steering law in order that CMG gimbals are commanded with respect to inertial coordinates.

The second term in the rightmost side of Eq. (2) is due to gimbal rotation, which re-orients the CMG rotors ($\underline{h}_i$), thus is able to produce changes in the magnitude and direction of the momentum stored in the CMG system. Its value can be controlled by adjusting the CMG gimbal rates, hence this term is used to establish a control torque. For an "ideal" double-gimballed CMG of the type sketched in Fig. 1, $\underline{\tau}_{ctl_i}$ has the form[1]:

$$\underline{\tau}_{ctl(i)}(\delta,\gamma) = -\left[\dot{\gamma}(\hat{\sigma}_\gamma(\delta) \times \underline{h}(\delta,\gamma)) + \dot{\delta}(\hat{\sigma}_\delta \times \underline{h}(\delta,\gamma))\right]_{(i)} \tag{3}$$

γ = Inner gimbal angle ($\dot{\gamma}$ is gimbal rate)
δ = Outer gimbal angle ($\dot{\delta}$ is gimbal rate)
$\underline{h}(\delta,\gamma)$ = Angular momentum of CMG at gimbal orientation (δ,γ)
$\hat{\sigma}_\gamma(\delta)$ = Unit vector along instantaneous inner gimbal axis
$\hat{\sigma}_\delta$ = Unit vector along outer gimbal axis

The purpose of the generic CMG "steering law" is to command a set of gimbal rates $(\dot{\delta},\dot{\gamma})$ such that the CMG control torque matches a desired value. Attitude control systems using CMGs are generally structured to possess more degrees of freedom (ie. more CMGs) than the minimum required for control purposes. "Optimal" CMG steering laws select a set of gimbal rates which attain the desired control torque while exploiting the extra degrees of freedom to avoid moving the CMG rotors and gimbals into undesirable configurations.

Torques arising from RCS jet firings can be likewise expressed:

$$\underline{\tau}_{jet_k} = -[(\underline{r}_k - \underline{r}_{cg}) \times \underline{T}_k] \tag{4}$$

$\underline{r}_k$ = Position of jet k
$\underline{T}_k$ = Thrust of jet k
$\underline{r}_{cg}$ = Position of spacecraft center of gravity

By applying jet and CMG torques during time intervals Δt, a vehicle rate change is produced:

$$[I]\underline{\Delta\omega}_s = \sum_{RCS} \underline{\tau}_{jet_k} \Delta t_k + \sum_{CMGs} \int_o^{\Delta t_i} \underline{\tau}_{IG_i}(\delta_i, \gamma_i)dt \tag{5}$$

$$+ \sum_{CMGs} \int_o^{\Delta t_j} \underline{\tau}_{OG_j}(\delta_j, \gamma_j)dt$$

$$\underline{\tau}_{IG_i}(\delta_i, \gamma_i) = -\dot{\gamma}_i[\hat{\sigma}_\gamma(\delta) \times \underline{h}(\delta, \gamma)]_{(i)}$$

$$\underline{\tau}_{OG_j}(\delta_j, \gamma_j) = -\dot{\delta}_j[\hat{\sigma}_\delta \times \underline{h}(\delta, \gamma)]_{(j)}$$

$[I]$ = Spacecraft Inertia Tensor

Over small gimbal displacements (ie. limited Δt) and assuming constant gimbal rates throughout the interval Δt, the CMG output torque does not exhibit large variation, hence the CMGs may be treated impulsively:

$$\underline{\Delta\omega}_s = [I]^{-1}\left[\sum_{RCS} \underline{\tau}_{jet_k} \Delta t_k + \sum_{CMGs} \underline{\tau}_{IG_i}(\delta_i, \gamma_i)\Delta t_i + \sum_{CMGs} \underline{\tau}_{OG_j}(\delta_i, \gamma_i)\Delta t_j\right] \tag{6}$$

Eq. (6) defines a rate change which is achieved by commanding a set of jet firing times (Δt_k) and CMG gimbal displacements (the angular displacements for inner and outer gimbals are respectively proportional to Δt_i and Δt_j). The three terms of Eq. 6 are used to formulate a set of activity vectors for linear selection.

RCS Jet:	CMG Inner Gimbal:	CMG Outer Gimbal
$\underline{A}_k = [I]^{-1}\underline{\tau}_{jet_k}$	$\underline{A}_i = [I]^{-1}\underline{\tau}_{IG_i}(\delta_i, \gamma_i)$	$\underline{A}_j = [I]^{-1}\underline{\tau}_{OG_j}(\delta_j, \gamma_j)$ (7)

A linear programming algorithm is used to determine a set of decision variables (Δt) which "optimally" command the actuators represented in Eq. (7) to deliver the vehicle rate change of Eq. (6). The linear programming problem is structured as stated below:

a) Minimize: $z = \sum_{n=1}^{N} c_n \left|(\Delta t)_n\right|$

b) Subject to: $\sum_{n=1}^{N} \underline{A}_n (\Delta t)_n = \underline{\Delta\omega}_s$ (8)

c) With: $-L_n < (\Delta t)_n < +U_n$

N = Total number of actuators (jets & CMG gimbals) in system.
c_n = Objective coefficent ("cost") associated with actuator n.

The equality constraint (Eq. 8b) is essentially Eq (6) with every active actuator considered in a single summation running over all activity vectors (Eq. 7). The decision variables (Δt) are restricted by the bounds imposed in Eq. (8c), which limit the amount of CMG gimbal displacement allowed over each selection. CMG gimbals are capable of rotating either "forward" or "backward", thus their decision variables Δt can become either positive or negative (creating two limits, $-L_n$ and $+U_n$, per variable). L_n is set to zero for RCS jets.

The linear programming process finds the solution to Eq. (8b) that minimizes the objective function (Eq. 8a) with decision variables constrained by the bounds of Eq. (8c). Since the decision variables for CMGs are allowed to go positive or negative, their corresponding c_n in Eq. (8a) actually take two values; one (c_n^+) representing the consequences of rotation in a positive sense, and another (c_n^-) for rotation in a negative sense. All such objective coefficients are positive quantities. The c_n which correspond to gimbal rotation in an unfavorable direction increase as the CMGs approach problematic orientations (as discussed below). By minimizing z, one chooses a solution which moves the CMGs to achieve the desired rate change (8b) while encouraging avoidance of undesired CMG configurations.

The c_n for RCS jets represent the penalty of using jets in the solution to Eq. (8b). By setting c_n much higher for jets than for typical CMGs, the latter devices are used exclusively whenever possible. These c_n are made proportional to the amount of fuel required per jet, thereby enabling the linear program to perform fuel-optimal jet selections.

Because the CMG rotor orientation changes as the gimbals are moving, the direction of the output torque (Eq. 3) correspondingly shifts, and the linearized solution to Eq. (8) gradually loses validity. In order to maintain the leading-order "impulsive" approximation to the output torque (in Eq. 6), updated selections (with re-calculated CMG activity vectors and objective coefficents) are performed after CMG gimbals have rotated through a pre-set angle (allowed maximum displacements of 5-10 degrees between selections were found to be adequate). Revised CMG

selections are also forced if CMG costs are found to increase significantly (indicating approach of a problematic state) while CMGs are in motion. In this fashion, the CMGs are moved to answer input requests and avoid undesired states over a series of instantaneously optimal linearized steps. A strategy of improving the global accuracy of the selection performed at each step is discussed in Ref. 1.

In order to simplify accomodation of RCS jets, the selection process of Eq. 8b is formulated as a vehicle rate-change request. This results in CMG decision variables representing gimbal angular displacements, leaving the absolute normalization of CMG gimbal rates as an effectively "free" parameter. In the simulation examples presented below, the CMG gimbal with the largest displacement was rotated at its peak rate, while other CMGs present in the solution were gimballed at lower rates (in relative proportion to their commanded angular displacements). This represents a "quickest" means of attaining the desired vehicle rate. Other strategies are also possible; CMG gimbal rates can be made proportional to their decision variables such that the vehicle is torqued less for smaller input requests. Methods of establishing gimbal rates are discussed in Ref. 1.

Peak gimbal rates are assumed in the calculation of activity vectors (Eq. 7). The CMG selection (Eq. 8) could easily be structured to solve a torque request by omitting gimbal rates from Eq. (7), and replacing $\underline{\Delta\omega_s}$ in Eq. (8) with the requested torque. The resultant solutions will then produce gimbal rates directly as decision variables.

The constants L_n and U_n in Eq. (8c) bound the amount of gimbal displacement allowed per selection in each respective direction. They are set to reflect the location of gimbal stops (if one made a change of variables to solve an input torque request, these bounds would directly represent peak gimbal rates). By appropriately decreasing these limits as input requests move the CMG system toward momentum saturation, the selection process accounts for the diminishing amount of momentum available to transfer into the "saturated" axis.

The optimal solution to the three-axis control problem of Eqs. (8a & 8b) (ignoring the bounds of Eq. 8c) will include only three linearly independent activity vectors (ie. only three CMG gimbals are selected to respond to requests). The upper bounds, however, place a limit to the output of each device, allowing the linear program to introduce as many activity vectors (ie. CMG gimbals) as needed to optimally provide the requested input.

The linear programming problem as stated in Eqs. (8) is solved by applying a version of the "Upper Bound Simplex" method[2], which has been modified[1] to allow selections of CMGs with positive and negative decision variables. The simplex selection process has been shown to effectively perform fuel-optimal jet selections[3]; an autopilot using this procedure has recently completed successful flight testing[4] on the Shuttle orbiter.

The application of linear programming to CMG selection produces an extremely flexible CMG steering law. Activity vectors representing linearized actuators (Eq. 7) are kept in a common pool which is scanned during each simplex selection. Actuator failures may be accomodated by preventing corresponding activity vectors from being selected by the simplex process (and eliminating the failed devices from the objective calculations). Since each CMG gimbal is modelled via an independent activity vector, single gimbals of dual-gimballed CMGs may be failed (ie. frozen at constant position), still leaving the surviving gimbal available for selection. Gimbal stops are represented by the bounds in Eq. (8c); these are considered directly in each simplex selection, and may be inserted, removed, or re-defined at any time. Peak gimbal rates and vehicle mass properties are represented by constants used in activity vector calculation, thus may be easily changed and updated. Since specific CMG mounting configurations are not assumed anywhere in the selection process, CMGs may be mounted in any orientation. The linear objective function (Eq. 8a) is optimized in each selection, eliminating the need of a separate "null motion" procedure to calculate gimbal rates which avoid problematic CMG orientations (null motion, if desired, may also be calculated directly under simplex by requesting a zero net rate change using a modified objective function, as demonstrated in Ref. 1). Finally, the simplex selection process is not limited to CMGs; other devices (such as RCS jets or reaction wheels) can be included, provided that they may be effectively represented by linearized activity vectors, objective coefficents, and upper bounds.

OBJECTIVE FUNCTION

The linear selection is performed to minimize the objective function evaluated in Eq. (8a). The objective factors (c_n) dictate the penalty of using a particular activity vector in the solution. The c_n for jets are set to large values corresponding to RCS fuel useage. The c_n for CMGs are generally much smaller, and are calculated as a sum of several components:

$$c_{j,s} = K_o + K_A F_{ANGLE}(j,s) + K_s G_{STOPS}(j,s) + K_L Y_{LINEUP}(j,s) \quad (9)$$

Activity vector j corresponds to CMG gimbal
s = Sense of rotation (+/-)

The K_o term is a small constant bias which keeps all $c_{j,s}$ non-zero. The remaining three terms reflect the configuration of the CMG system and are independently discussed below. The balance between the factors K_A,K_s, and K_L determine the relative amount by which their respective effects are accounted for in the objective function. Each of these terms possesses two values per gimbal corresponding to forward and backward rotation.

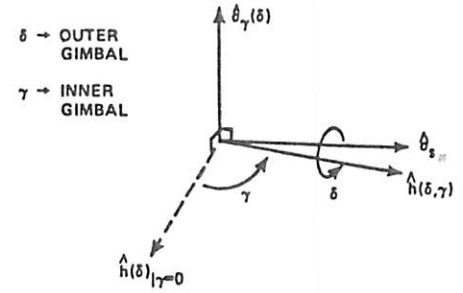

Outer gimbal control of 2-DOF CMG is degraded severely if inner gimbal angle γ approaches ±90° and CMG rotor $h(\delta, \gamma)$ aligns with outer gimbal axis σ_δ:

→ Select CMGs to minimize inner gimbal angles

Figure 2

When the inner gimbal angle of a double-gimballed CMG approaches +/-90° (as portrayed in Fig. 2), the CMG rotor nears alignment with the outer gimbal axis. The control authority of the outer gimbal thus decreases with the cosine of the inner gimbal angle (as seen in Eq. (3) via the $\hat{\sigma}_\delta \times \underline{h}(\delta,\gamma)$ factor governing the outer gimbal torque). In order to maintain outer gimbal control authority, the CMGs are steered to avoid encountering excessive inner gimbal angles. This is the purpose of the F_{ANGLE} term as included in Eq. (9):

$$F_{ANGLE}(j,s) = \begin{cases} |\gamma_j| & \text{If j = inner gimbal and rotation "s" increases } |\gamma_j|. \\ 0 & \text{Otherwise} \end{cases} \tag{10}$$

Inner gimbal rotations which increase the magnitude of the inner gimbal angle $|\gamma_j|$ are assigned a cost contribution in direct proportion to the current value of $|\gamma_j|$. Rotations which decrease $|\gamma_j|$ (or outer gimbal rotations which have no effect on γ_j) are given no cost contributions via F_{ANGLE}. Rotations that increase the inner gimbal angle become linearly more expensive as the angle grows. Solutions involving the activity vector and decision variable that bring $|\gamma_j|$ back to zero thus become increasingly favored as $|\gamma_j|$ rises.

The G_{STOPS} function produces an amplitude which signals a "warning" to the selection procedure as a CMG gimbal nears a stop. In contrast to the linear form of F_{ANGLE}, G_{STOPS} contributes a nearly insignificant amount to the objective if the gimbal is far from its stop (allowing the other terms in Eq. 30b to act unimpeded), but increases rapidly as the gimbal approaches a pre-set distance from the stop location.

$$G_{STOPS}(j,s) = \begin{cases} \Lambda\left[\dfrac{\theta_j}{\theta_S(j,s)}\right] & \text{If stops are present on gimbal \#j, and rotation "s" moves CMG toward stop.} \\ 0 & \text{Otherwise....} \end{cases} \tag{11}$$

θ_j = Gimbal angle (ie. δ_j or γ_j)

$\theta_S(j,s)$ = Stop position on gimbal j, sense s

The function Λ (see Ref. 1) contributes neglibly for low θ_j, however as θ_j/θ_S approaches unity, Λ diverges steeply. If the rotation "s" brings a CMG toward an existing gimbal stop, the objective contribution will be proportional to Λ. No such contribution will be added to the objective coefficent if a gimbal either has unlimited freedom or rotation "s" will remove it from a stop. If a CMG gimbal has neared its stop, the function Λ will contribute appreciably, and solutions which rotate the CMG away from the stop are heavily favored over those which move it closer.

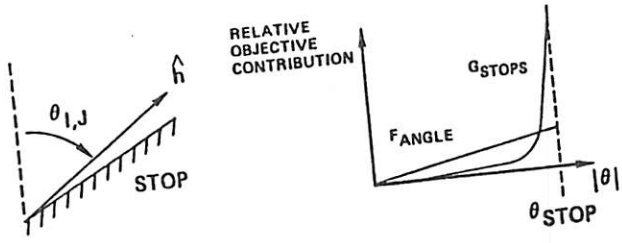

FIGURE 3: RELATIVE CONTRIBUTION OF F_{ANGLE} AND G_{STOPS} TO OBJECTIVE VS. θ

The G_{STOPS} and F_{ANGLE} functions are plotted together as a function of gimbal angle in Fig. 3 for a rotation which moves a CMG toward a stop. F_{ANGLE} dominates initially at low θ, encouraging a return to zero displacement via a linearly increasing objective coefficent. As the gimbal stop is approached, G_{STOPS} dominates, and solutions which move the CMG further in that direction become highly discouraged.

Since the output torque of a CMG is always perpendicular to its rotor, a CMG is unable to produce a torque along the rotor axis (aside from altering the rotor rate, but this is held constant and not considered a control variable). If two CMGs are aligned with their rotors parallel or antiparallel, control along the direction of the alignment must be performed exclusively with the remaining devices in the system, which can degrade the 3-axis control capability of the CMG configuration. Internal singular states (ie. CMG orientations removed from saturation which suffer a loss of control about at least one axis) of double-gimballed CMG systems are always related to CMG rotor alignments. In order to maintain a high level of three-axis controllability, the rotors of double-gimballed CMG systems are conventionally steered away from either parallel or antiparallel alignments. This is encouraged by the Y_{LINEUP} factor as included in Eq. (9).

The terms discussed above (F_{ANGLE} and G_{STOPS}) assign cost contributions to the objective coefficents of an activity vector which depend only on the corresponding gimbal angle. They do not account for the orientation of a CMG rotor with respect to other CMGs. The term (Y_{LINEUP}) that is discussed here differs considerably in that it expresses an amplitude which drives the CMG under consideration to avoid parallel or antiparallel alignment with other CMGs in the system.

$$Y_{LINEUP}(j,s) = Y_o(j,s) + B \qquad (12)$$

Where:

$$Y_o(j,s) = \sum_{I=1}^{R\ (I\neq J)} SG(I,j,s)\ m(I,J)$$

R = Number of CMG rotors in system

J = Rotor index associated with CMG gimbal #j.

Note: The sum runs over all CMG rotors except that associated with gimbal #j. Uppercase variables denote CMG rotors (ie. J), whereas lowercase variables denote CMG gimbals (ie. j).

m(I,J) = "Urgency" of lineup condition (increases as rotors I and J approach one another).

$$SG(I,j,s) = \begin{cases} +1 \text{ if rotation "s" moves rotor J toward rotor I} \\ -1 \text{ if rotation "s" moves rotor J away from rotor I} \end{cases}$$

B = Bias to keep all $Y_{LINEUP}(j,s)$ non-negative (ie. $B = -\min Y_o(j,s)$)

Eq. 12 defines the antilineup function Y_{LINEUP}. The Y_o term is a sum of amplitudes which reflect the lineup condition of the CMG rotor in question (#J) with respect to the other rotors in the system. If the rotation "s" of gimbal #j moves the associated CMG rotor toward parallel or antiparallel alignment with another rotor in the system (#I), the "SG(I,j,s)" flag will be positive; if the rotation moves the rotors mutually apart, "SG" will be negative. The "m" factor describes the "urgency" of the lineup condition; ie. m(I,J) equals zero if the two CMGs in question are mutually perpendicular and linearly increases as the rotors approach one another, reaching a maximum at parallel or anti-parallel alignment. The products of "SG" and "m" are evaluated for the rotor and gimbal under consideration paired with all other rotors in the system; these are summed to form $Y_o(j,s)$.

The value of $Y_o(j,s)$ quantitatively represents the consequence of moving CMG gimbal #j in direction "s", with respect to lineup with other CMGs in the system. A positive $Y_o(j,s)$ indicates approaching lineup, and the magnitude of Y_o indicates the degree of alignment. The opposite rotation will have the inverse consequence; ie. the $Y_o(j,-s)$ will be negative with equal magnitude, indicating the direction in which to move gimbal #j to escape alignment. Since negative objective values can yield unphysical solutions, a bias must be added onto Y_o in order to keep all Y_{LINEUP} non-negative. This bias (B) is the negative of

the minimum $Y_o(j,s)$ over all j and s; the $Y_{LINEUP}(j,s)$ will thus range from zero (ie. gimbal rotation with minimum $Y_o(j,s)$) on up. Simplex is thus encouraged to select the lower cost activity vectors corresponding to gimbal rotation which moves the rotors away from lineups; this selection is increasingly favored as rotor alignments are approached.

The Y_{LINEUP} function defined above uses an instantaneous approximation to the CMG rotation and does not consider the motion of one CMG with respect to another (these factors can not be directly accounted for under a linear selection). CMGs are encouraged via Y_{LINEUP} to move independently away from one another; this strategy is found to be very effective in managing system redundancy to avoid rotor alignment, as will be illustrated in the simulation examples.

Steering single gimballed CMG systems away from lineup conditions is generally not adequate for avoiding singular orientations. Objective contributions which address the needs of single gimballed CMGs are discussed in Ref. 1.

HYBRID RCS/CMG SOLUTIONS

Because of their much higher objective values, RCS jets are not selected by simplex unless translational control is desired, or CMGs are unable to respond due to effective saturation. Since the jets are so expensive and have much more control authority, the hybrid solutions to rotational requests often consist of very short RCS pulses coupled with extensive CMG activity. Such solutions are unphysical and problematic for several reasons, ie. nonlinearities introduced as CMGs gimbal over large angles, and the minimum limits conventionally imposed on the duration of RCS pulses. These solutions also result in the transfer of all CMG momentum before resorting primarily to the RCS system (which leaves the CMGs momentum saturated upon finishing the operation; certainly an undesired feature). Non-negligible attitude errors can also occur under these realizations of hybrid maneuvers; RCS firings can deliver a momentum impulse very quickly (ie. on-time of the jets concerned), whereas extensive CMG motion requires a considerably larger interval as the CMGs gimbal over sizable angles to transfer the extra momentum needed to complete the request. Significant attitude errors can accumulate during the period between completion of the RCS firing and acquisition of the desired CMG state.

These difficulties are avoided by repeating the linear selection whenever jets and CMGs have been specified together in the original simplex solution. The second selection is performed with considerably reduced upper bounds on CMG gimbal displacement and lower RCS objective "costs". The maximum allowed gimbal displacement puts a ceiling on the amount of CMG involvement in answering the input request; by reducing this quantity, we restrict the CMGs from moving over large angles and limit the influence of nonlinear effects. CMGs are thus confined to a "trimming" role, and the primary maneuver is performed by "solid" RCS firings (with non-trivial on-times).

In contrast to the much larger RCS cost, all CMGs appeared similarly priced in the original selection, and CMG useage did not discriminate between "favorable" and "unfavorable" rotations. In the second selection, the RCS cost is adjusted to the current mean CMG cost (after accounting for the reduced CMG control authority), thus the "cheaper" CMGs are encouraged to be used along with RCS firings. This results in an effective "desaturation" tendency, where hybrid RCS/CMG operations often leave the CMGs in a lower cost (ie. more favorable) orientation.

When the CMG system is removed from saturation, finite upper bounds are still maintained on gimbal displacement. If a large rotational request is input to the selection procedure, those bounds can encourage the introduction of RCS jets (even when the CMG system is unsaturated), which can instigate a re-selection (as discussed above) that prevents the CMGs from extensively responding to a request which would bring them into saturation.

By allowing the magnitudes of RCS costs and CMG upper bounds to decrease with the approach of the CMG system to saturation, the primary selection may prove directly realizable and the need for the additional hybrid selection may be eliminated.

A straightforward means of performing hybrid selections which fire jets in order to move CMGs away from saturation and into superior orientations (while holding constant vehicle rates) has been demonstrated[1] by enabling jets to be selected along with CMGs in the simplex-based null motion process.

SIMULATION EXAMPLES

In order to test the performance of the hybrid selection/steering procedure, it has been interfaced to a closed-loop control system based upon the OEX Advanced Autopilot.[3,4] This autopilot incorporates a phase-space control law, which derives vehicle rate-change commands from a weighted sum of vehicle attitude and rate errors, providing coordinated control of vehicle rotational states. Mass properties of the power tower space station[5] (without orbiter or payloads attached) have been assumed in these simulations.

In the first tests, a quad double-gimballed CMG configuration is used (as depicted in Fig. 4). This mounting style was derived from the convention used in Skylab[6] (three CMGs initially perpendicular), with a fourth added skewed at equal angles to each of the others. This configuration is not proposed as an optimal CMG mounting protocol for the space station; the hybrid steering law is easily amenable to any CMG arrangement (including parallel mounting[7]). The CMGs are modelled in accordance with recent specifications proposed for the space station[8], ie. an angular momentum capacity of 3500 ft-lb-sec per rotor, and peak gimbal rates of 5 deg/sec on both inner and outer gimbals. Stops are imposed at +/-90° on inner gimbal travel, and the outer gimbal is

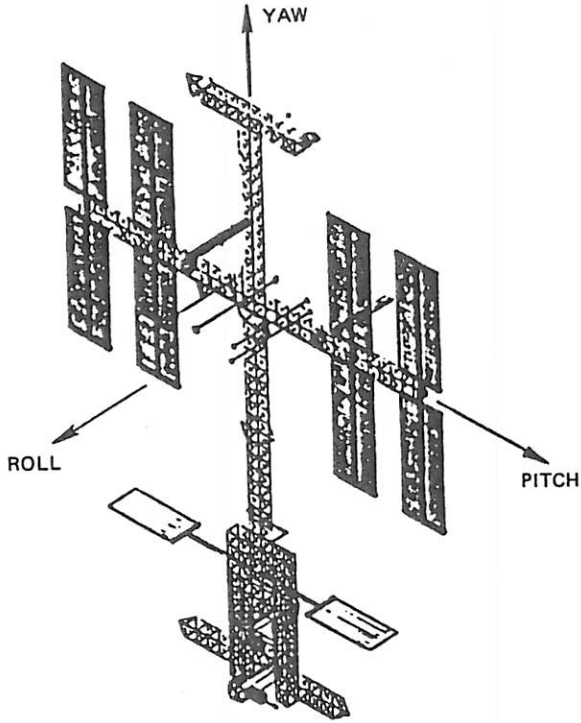

Fig. 4. (a) POWER TOWER SPACE STATION

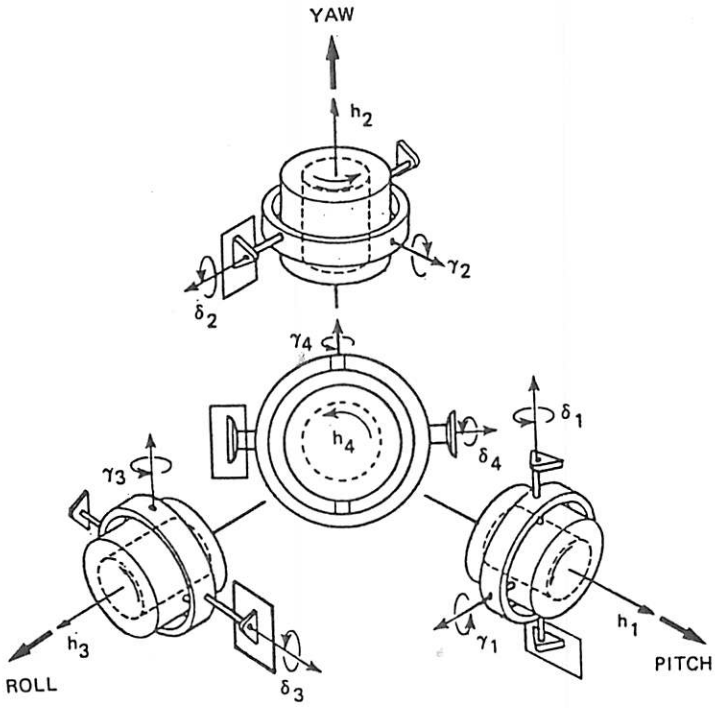

Fig. 4. (b) INITIAL CMG ORIENTATION

assumed capable of continuous rotation. "Ideal" CMGs are assumed in the simulation, and higher-order dynamic effects (eg. gimbal acceleration torques, servo effects, etc.) are not currently included. The control procedure normalizes the CMG gimbal displacements in the simplex solutions to the peak gimbal rates in order to promptly realize the commanded vehicle rates (smoother gimbal motion may be obtained by making gimbal rates proportional to their corresponding absolute displacements; see Ref. 1).

The power tower is assumed to possess 12 RCS jets, which operate at a nominal thrust of 75 lb each, and are clustered into mutually orthogonal triads located at four positions on the spacecraft (see Ref. 5). Jets are assumed to be discrete devices, and firings are rounded to the closest 80 msec increment. No separate logic is used to introduce jets; they are prescribed and selected by simplex as discussed above.

All tests are performed in an inertial environment; Euler coupling and the interaction of vehicle rates with CMG momentum (Eq. 2) are included as disturbances, while aerodynamic and gravity gradient torques, which would be present on-orbit, are ignored. Vehicle rates are initialized to zero at the start of each test.

The first example commands a series of rate increases (0.003 deg/sec each) about the vehicle pitch and roll axes (the yaw rate is held at zero). Five such increases are requested, building net rates of 0.015 deg/sec over the 100 sec duration of the test run. This is a significant rate, considering the sizable vehicle inertias ($10^6 \rightarrow 10^7$ slug-ft^2) and limited CMG control authority. Two test cases are considered; one with a complete objective function (Eq. 9), and another without including the antilineup component (ie. K_L=0).

Gimbal angles for both cases are shown in Fig. 5. Results using a complete objective are shown in the left column; both inner and outer gimbal systems are seen to be employed in answering requests (excessive inner gimbal swings are avoided), and jets are required to complete maneuvers (as indicated by asterisks) toward the end of the run. The results for the test omitting the antilineup component are shown in the right column. The remaining objective components work only to minimize the inner gimbal angles, and this is indeed what is noted in Fig. 5c; the inner gimbals are hardly used until they are required to complete requests at the conclusion of the test.

CMG rotor alignments are portrayed in the upper portion of Fig. 6. The complements of the relative angles between all possible CMG rotor pairs are plotted (there are 6 combinations of pairs possible in a 4-CMG system). A parallel lineup is indicated when a curve nears +90°, an antiparallel lineup is indicated when a curve nears -90°, and the respective CMG rotors are orthogonal (the "ideal" case) when the curve is in proximity to zero. When using the complete objective function (Fig. 6a), CMGs are generally seen to avoid alignment until all move together toward saturation at the close of the test. When lineup avoidance is not considered in the objective (Fig. 6b), CMG rotors are

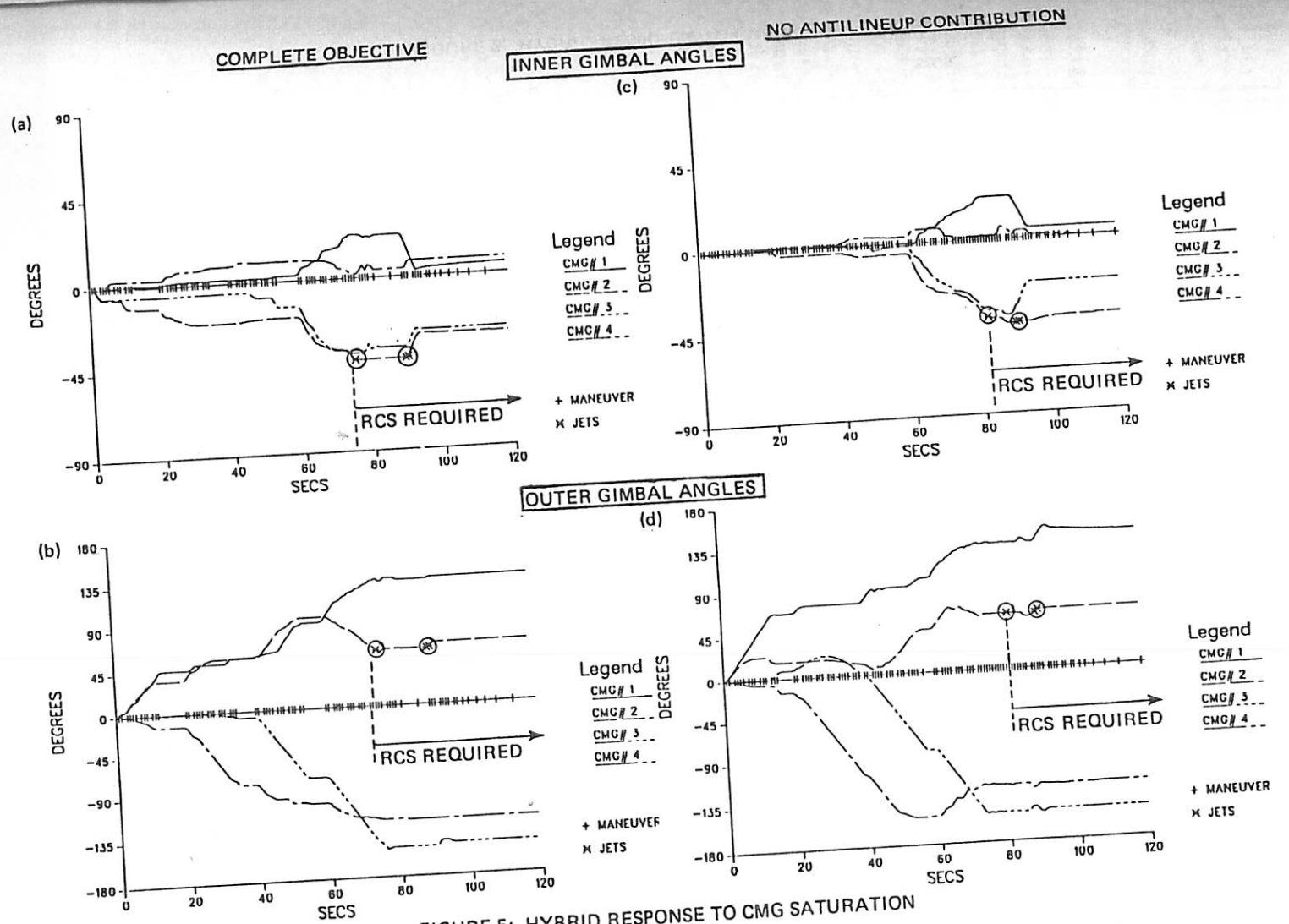

FIGURE 5: HYBRID RESPONSE TO CMG SATURATION

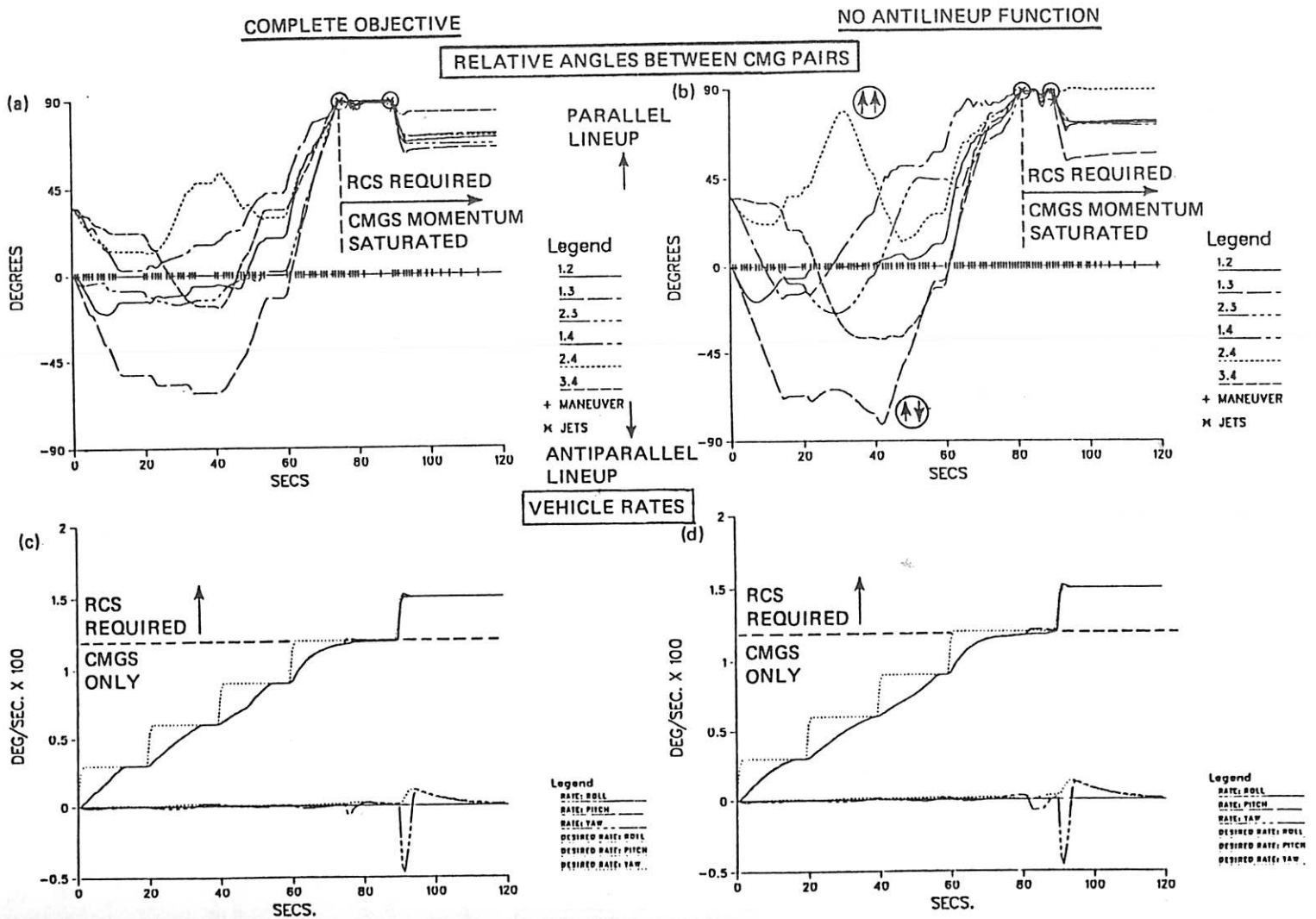

FIGURE 6: HYBRID RESPONSE TO CMG SATURATION

seen to more frequently approach alignment; at the positions indicated on the plot, rotor pairs moved within 10° of parallel and antiparallel alignment before saturation was reached. The extreme minimization of inner gimbal angles attained in this case was performed at the expense of avoiding interim CMG rotor alignments. In both test cases, jets were automatically selected by simplex when continued CMG performance was inhibited due to momentum saturation.

Vehicle rates are plotted in the lower portion of Fig. 6. The commanded input about the pitch and roll axes is plotted as the dotted "staircase"; the vehicle rates (solid lines) are seen to follow this input. Since the 3-axis control authority is generally higher, a quicker vehicle response is noted in the run incorporating the complete objective function. The last requested rate increase occurs after the CMGs have reached momentum saturation, hence it is answered primarily via an RCS response; due to their greater control authority, the vehicle is seen to respond more rapidly when jets are employed. The vehicle is commanded to maintain a constant yaw attitude while rates are built around the other axes. A small yaw disturbance is encountered when jets participate in maneuvers (the moment of inertia is an order of magnitude smaller in this coordinate), however it is easily compensated by the phase space controller.

The next test uses a 5-CMG array; four are included as depicted in Fig. 4, and a fifth "skewed" CMG is added perpendicular to CMG #4. The command sequence consists of two rate-change requests followed by attitude holds. The initial segment requests 0.03 deg/sec about the pitch axis, and enters attitude hold after 30 sec have elapsed. Once the desired attitude has been acquired, a rate of 0.005 deg/sec is requested about the roll axis. All CMG outer gimbals are failed after this rate is achieved, thus subsequent CMG control must be realized exclusively with inner gimbals. After keeping the commanded rate for approx. 60 sec, an attitude hold is commanded, and rates are again brought to zero.

Results are given in Fig. 7. Gimbal angles are plotted in the left column; note that jets were introduced to establish and remove the commanded 0.03 deg/sec pitch rate. Since the CMG array (as mounted and initialized in this configuration) can only provide enough momentum to achieve approx. 0.015 deg/sec along this axis, jets are required to reach the desired value of 0.03 deg/sec. Because of the restrictive upper bounds placed upon CMG gimbal displacement in solutions including jets (as described earlier), CMG participation is limited in responding to this request, and the bulk of maneuvering is accomplished via the RCS. This prevents the CMGs from being first driven into saturation before introducing jets; the hybrid response to such a large input request favors an RCS-based solution in order that the CMGs are not saturated when the final state is achieved.

Vehicle rates are given in Fig. 7c. The 0.03 deg/sec request is seen to be quickly established (A) and removed (B) primarily via jets. In order to restore the desired attitude, the vehicle coasts at approx. -0.002

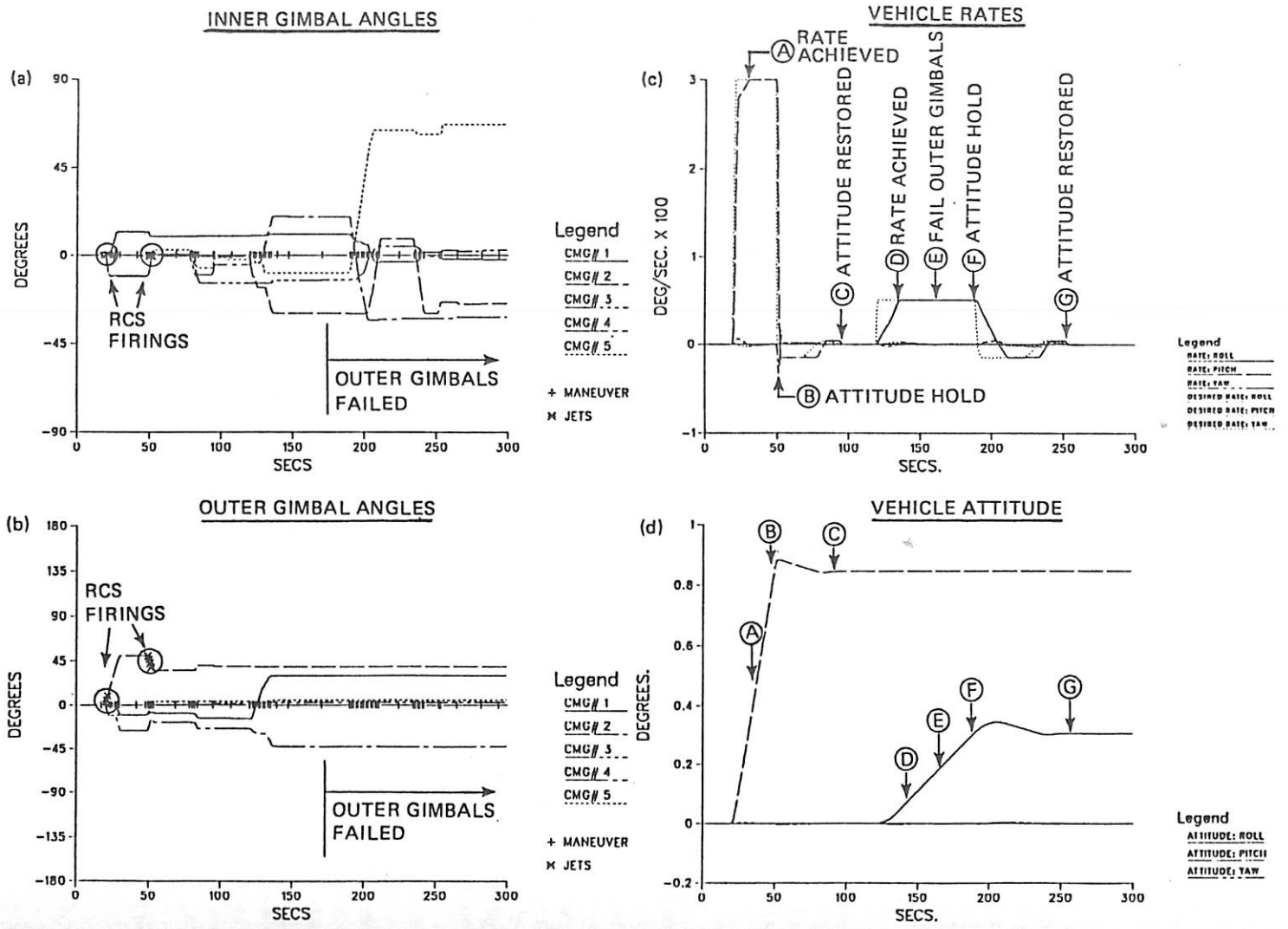

FIGURE 7: HYBRID RESPONSE TO LARGE REQUESTS AND GIMBAL FAILURES

deg/sec after the attitude hold is commanded; this rate is removed and the vehicle is stabilized (C) entirely via the CMG system (0.002 deg/sec is well within the CMG control margin).

After vehicle rates have damped to zero, a 0.005 deg/sec rate is requested about the roll axis. This is handled exclusively by the CMGs, and no jets are required (see Figs. 7a & b). After this rate is achieved (D), the outer gimbals of all CMGs are failed (ie. frozen at constant position and inhibited from selection [E]), and an attitude hold is commanded (F). As seen in Figs. 7a & b, this was achieved entirely via the inner gimbal system, no RCS assistance was required. At point G, vehicle attitude was restored, and rates were returned to zero.

Vehicle attitudes are plotted in Fig. 7d. The command sequence executed in this test established attitude changes of approx. 0.85° in pitch and 0.3° in roll. Yaw attitude remains at zero, as commanded.

The set of activity vectors available for simplex selection can easily be re-defined and restricted, as illustrated by the single-gimbal failures performed in this example. Effective singularity avoidance in the resulting single gimballed CMG system can not be achieved by merely steering away from rotor alignments; modifications to the objective which address this problem are outlined in Ref. 1.

CONCLUSION

The adaptation of linear programming to command CMG systems has produced an extremely flexible CMG steering procedure; it is able to successfully establish control using an array of double gimballed CMGs mounted in different orientations, and effectively manage truncated CMG systems resulting from various failure modes. The composite objective function encourages CMG selections that avoid gimbal stops, excessive inner gimbal swings, and rotor alignments.

The hybrid procedure has also performed optimal jet selections, and has been shown to be effective in addressing mixed CMG/RCS maneuvers. The adoption of upper bounds in the CMG selection process directly accounts for gimbal stops, and places an effective limit upon allowed CMG control authority; RCS jets have been seen to be automatically introduced in response to requests which can not be answered via CMGs alone.

ACKNOWLEDGEMENTS

The author wishes to express his sincere thanks to Edward V. Bergmann for helpful discussions and advice. This work was preformed under C.S. Draper Laboratory Independent Research and Development Project #207.

REFERENCES

1) J.A. Paradiso, "A Highly Adaptable Steering/Selection Procedure for Combined CMG/RCS Spacecraft Control; Detailed Report," C.S. Draper Lab. Report CSDL-R-1835, Feb., 1986.

2) S.P. Bradley, A.C. Hax, T.L. Magnanti, Applied Mathematical Programming, Addison-Wesley Publishing Co., Reading, MA., 1977.

3) E.V. Bergmann, S.R. Croopnick, J.J. Turkovich, C.C. Work, "An Advanced Spacecraft Autopilot Concept," Journ. of Guidance and Control, Vol. 2, No. 3, May/June 1979, p. 161.

4) This autopilot was flight-tested on Space Shuttle missions STS 51G (June, 1985) and STS 61B (Nov., 1985).

5) "Space Station Reference Configuration Description," NASA/JSC, JSC-19989, August 1984.

6) Skylab Program Operational Data Book Vols. II and IV, NASA MSC-01549, 1971.

7) H.F. Kennel, "Steering Law For Parallel Mounted Double-Gimballed Control Moment Gyros - Revision A," NASA TM-82390, Jan. 1981.

8) "Space Station Advanced Development Control Moment Gyro (CMG) Data," NASA MSFC memo ED15-85-43, July, 1985.